Aging Cell (2011) pp1–18 Doi: 10.1111/j.1474-9726.2011.00700.x

The telomerase activator TA-65 elongates short telomeres and increases health span of adult/old mice without increasing cancer incidence

Bruno Bernardes de Jesus,[1] Kerstin Schneeberger,[1] Elsa Vera,[1,2] Agueda Tejera,[1] Calvin B. Harley[3] and Maria A. Blasco[1]

[1]Telomeres and Telomerase Group, Molecular Oncology Program, Spanish National Cancer Centre, Melchor Fernández Almagro 3, Madrid E-28029, Spain
[2]Life Length, Agustín de Betancourt 21, Madrid E-28003, Spain
[3]Telome Health, Menlo Park, CA 94025, USA

Summary

Here, we show that a small-molecule activator of telomerase (TA-65) purified from the root of *Astragalus membranaceus* is capable of increasing average telomere length and decreasing the percentage of critically short telomeres and of DNA damage in haploinsufficient mouse embryonic fibroblasts (MEFs) that harbor critically short telomeres and a single copy of the telomerase RNA *Terc* gene (G3 *Terc*$^{+/-}$ MEFs). Importantly, TA-65 does not cause telomere elongation or rescues DNA damage in similarly treated telomerase-deficient G3 *Terc*$^{-/-}$ littermate MEFs. These results indicate that TA-65 treatment results in telomerase-dependent elongation of short telomeres and rescue of associated DNA damage, thus demonstrating that TA-65 mechanism of action is through the telomerase pathway. In addition, we demonstrate that TA-65 is capable of increasing mouse telomerase reverse transcriptase levels in some mouse tissues and elongating critically short telomeres when supplemented as part of a standard diet in mice. Finally, TA-65 dietary supplementation in female mice leads to an improvement of certain health-span indicators including glucose tolerance, osteoporosis and skin fitness, without significantly increasing global cancer incidence.

Key words: telomerase activation; TA-65; telomere length; aging; mouse.

Introduction

Progressive attrition of telomeres is one of the best understood molecular changes associated with organismal aging in humans (Harley *et al.*, 1990) and in mice (Flores *et al.*, 2008). Telomeres are specialized structures at the ends of chromosomes, with an essential role in protecting the chromosome ends from fusions and degradation (Blackburn, 2001; de Lange, 2005). Mammalian telomeres consist of TTAGGG repeats bound by a six-protein complex known as shelterin (de Lange, 2005). A minimum length of TTAGGG repeats and the integrity of the shelterin complex are necessary for telomere protection (Blackburn, 2001; de Lange, 2005). Telomerase is a cellular reverse transcriptase (TERT, telomerase reverse transcriptase) capable of compensating telomere attrition through *de novo* addition of TTAGGG repeats onto the chromosome ends by using an associated RNA component as template (*Terc*, telomerase RNA component) (Greider & Blackburn, 1985). Telomerase expression can be detected in a number of adult cell types, including peripheral lymphocytes and adult stem cell compartments; however, this is not sufficient to maintain telomere length with age in most human and mouse tissues (Blasco *et al.*, 1997; Harley, 2005; Flores *et al.*, 2008). Further supporting the notion that telomerase levels may be rate-limiting for organismal aging, some diseases characterized by premature loss of tissue renewal and premature death, such as *dyskeratosis congenita*, *aplastic anemia* and *idiopathic pulmonary fibrosis*, are linked to germline mutations in *Tert* and *Terc* genes, which result in decreased telomerase activity and accelerated telomere shortening (Mitchell *et al.*, 1999; Vulliamy *et al.*, 2001; Yamaguchi *et al.*, 2005; Armanios *et al.*, 2007; Tsakiri *et al.*, 2007). A role for telomerase in tissue renewal and organismal lifespan is also supported by telomerase-deficient (*Terc*$^{-/-}$) mice (Blasco *et al.*, 1997). These mice show progressive telomere shortening from the first generation (G1) until the third (G3) or fourth (G4) generation when in a pure C57BL6 background by which stage they present critically short telomeres, defective stem cell proliferative capacity, infertility because of germ cell apoptosis and increased genomic instability (Blasco *et al.*, 1997; Herrera *et al.*, 1999; Flores *et al.*, 2005). We and others have shown that restoration of telomerase activity in these mice, by reintroduction of one copy of the *Terc* gene, rescues critically short telomeres and reverses chromosomal instability and cell and tissue defects associated with late-generation telomerase deficiency, including rescue of stem cell dysfunction and of organismal lifespan (Hemann *et al.*, 2001a; Samper *et al.*, 2001a; Siegl-Cachedenier *et al.*, 2007). These studies illustrate that telomerase is preferentially recruited to the shortest telomeres, similarly to that shown for budding yeast (Teixeira *et al.*, 2004), thereby ensuring chromosomal stability and tissue fitness. Importantly, these findings also suggested that therapies aimed to re-activate telomerase and

Correspondence
Maria A. Blasco, Telomeres and Telomerase Group, Molecular Oncology Program, Spanish National Cancer Centre, Melchor Fernández Almagro 3, Madrid, E-28029, Spain. Tel.: +?????????; fax: +????????????; e-mail: mblasco@cnio.es

Accepted for publication *9th February 2011*

ACEL 700 B | Dispatch: 28.3.11 | Journal: ACEL | CE: Sindhuja | Journal Name | Manuscript No. | Author Received: | No. of pages: 18 | PE: Ramya

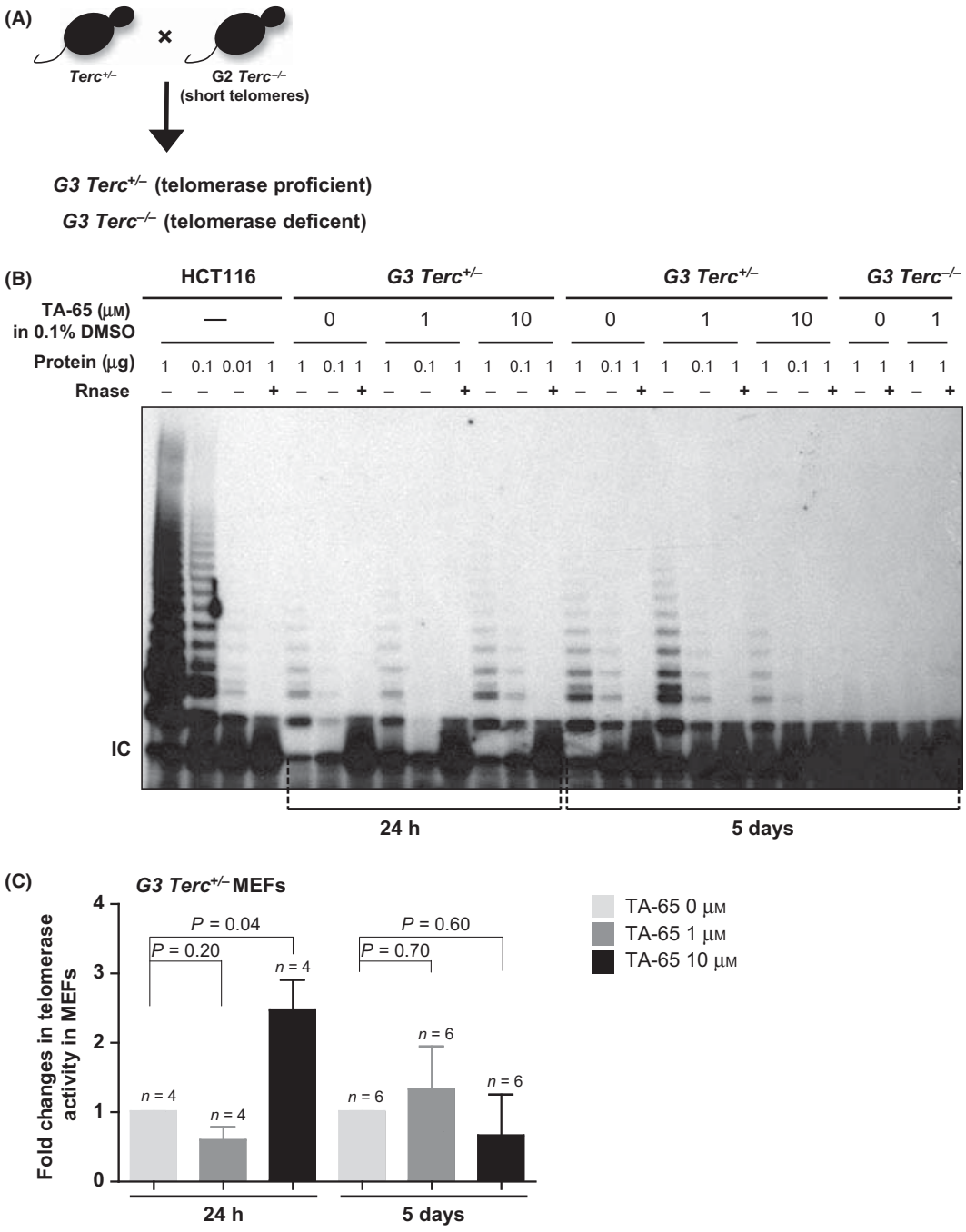

COLOR

Fig. 1 TA-65 rescues short telomeres in a telomerase-dependent manner. (A) Scheme of mouse crosses. (B) Telomerase activity was measured in mouse embryonic fibroblasts (MEFs) extracts grown in the presence or absence of TA-65 for 24 h and 5 days. The indicated concentrations of TA-65 were tested. A cellular extract from HCT116 cells was included as a positive control, and RNase was added in all experimental settings as negative control. IC, PCR efficiency control. (C) Quantification of telomere repeat amplification protocol assay values is expressed in fold changes of TA-65-treated cells compared to DMSO-treated controls. At least four independent experiments were used per condition. The mean amounts of telomerase activity and error bars (standard deviation) in the different experimental settings are shown. One-way ANOVA was used for statistical analysis. (D, E) Telomere fluorescence determined by Quantitative telomere fluorescence *in situ* hybridization on MEFs from the indicated genotypes grown in different concentrations of TA-65. Histograms represent the frequency of telomere fluorescence in Kb per telomere dot from a total of 50 nuclei, representing at least 650 telomeric dots per genotype. The red line indicates telomeres presenting < 20 kb of size. (F, G) Comparison of the percentage of 'signal-free' ends and short telomeres (< 8 kb) in control DMSO-treated MEFs of different genotypes. Student's *t*-test was used for statistical comparisons. (H) Comparison of the percentage of 'signal-free' ends and short telomeres (< 8 kb) between MEFs of different genotypes. Student's *t*-test was used for statistical comparisons. (I) Mean γ-H2AX immunofluorescence (green) per nucleus of MEFs of the indicated genotype, in the presence or absence TA-65 treatment for 5 days (DAPI in blue; at least 200 nucleus were scored per condition). Quantitative image analysis was performed using the Definiens Developer Cell software (version XD 1.2; Definiens AG). (J) Representative immunofluorescence images showing the γ-H2AX (green) and nucleus staining (DAPI - Blue), in the indicated genotypes.

COLOR

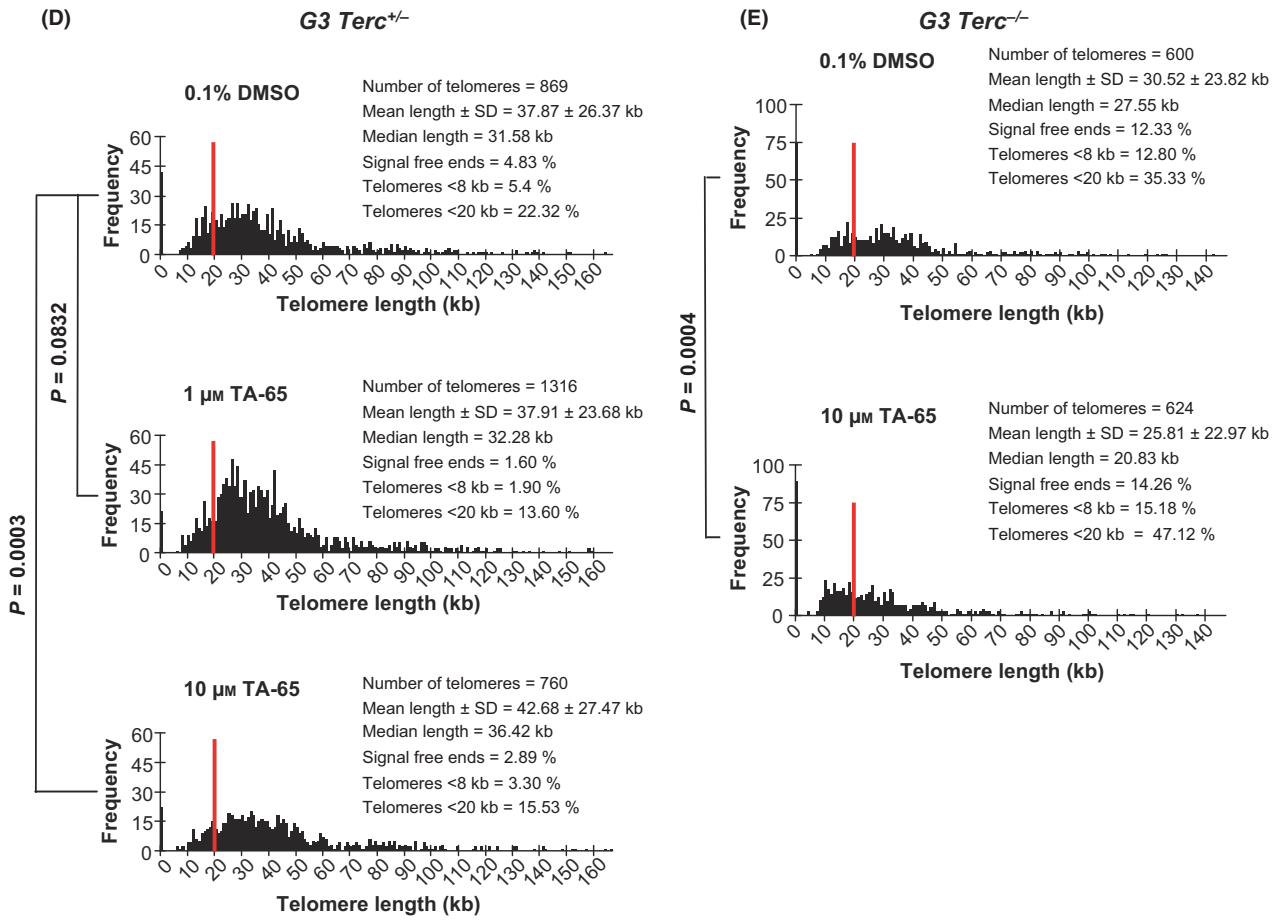

Fig. 1 Continued.

elongate short telomeres with age could have significant anti-aging effects. In this regard, we recently demonstrated that enhanced telomerase activity in mice overexpressing TERT is able to delay aging and extent the median lifespan by 40%, when combined with increased cancer resistance (Tomas-Loba *et al.*, 2008).

Here, we report on our initial findings on the mechanism of action of TA-65, a small-molecule telomerase activator derived from an extract of a plant commonly used in traditional Chinese medicine, *Astragalus membranaceous*. TA-65 was identified in an empirical screen based on its ability to upregulate basal telomerase activity levels in neonatal human keratinocytes and has been studied in humans as a dietary supplement (Harley *et al.*, 2010) leading to a decline of senescent and natural killer cells together with a significant reduction in the percentage of cells with short telomeres. Telomerase activation data and functional studies on a related molecule from this plant have been recently reported (Fauce *et al.*, 2008). In that study, human immune cells were exposed *ex vivo* to the activator, and this resulted in significant telomere elongation and enhanced proliferative capacity of these cells. Here, we demonstrate that TA-65 is capable of increasing telomerase activity and elongating critically short telomeres in a telomerase-dependent manner in mouse embryonic fibroblasts (MEFs) haploinsufficient for the telomerase RNA component and *in vivo*, when supplemented as part of a standard diet in mice. We also report initial findings on the outcomes of a TA-65 dietary supplementation in female mice, and how it leads to an improvement of certain health-span indicators. Importantly, treatment with TA-65 did not show any detectable negative secondary effects, including no increase in the incidence of cancer.

Results

TA-65 stimulates telomerase activity and leads to telomerase-dependent elongation of short telomeres and rescue of DNA damage in MEF haploinsufficient for the telomerase RNA component

TA-65 has been identified as an effective telomerase activator in human immune cells, and neonatal keratinocytes and fibroblasts (Fauce *et al.*, 2008; Harley *et al.*, 2010). To delineate whether TA-65 could also have an impact on telomerase-dependent telomere extension, we tested its capacity to affect the length of

COLOR

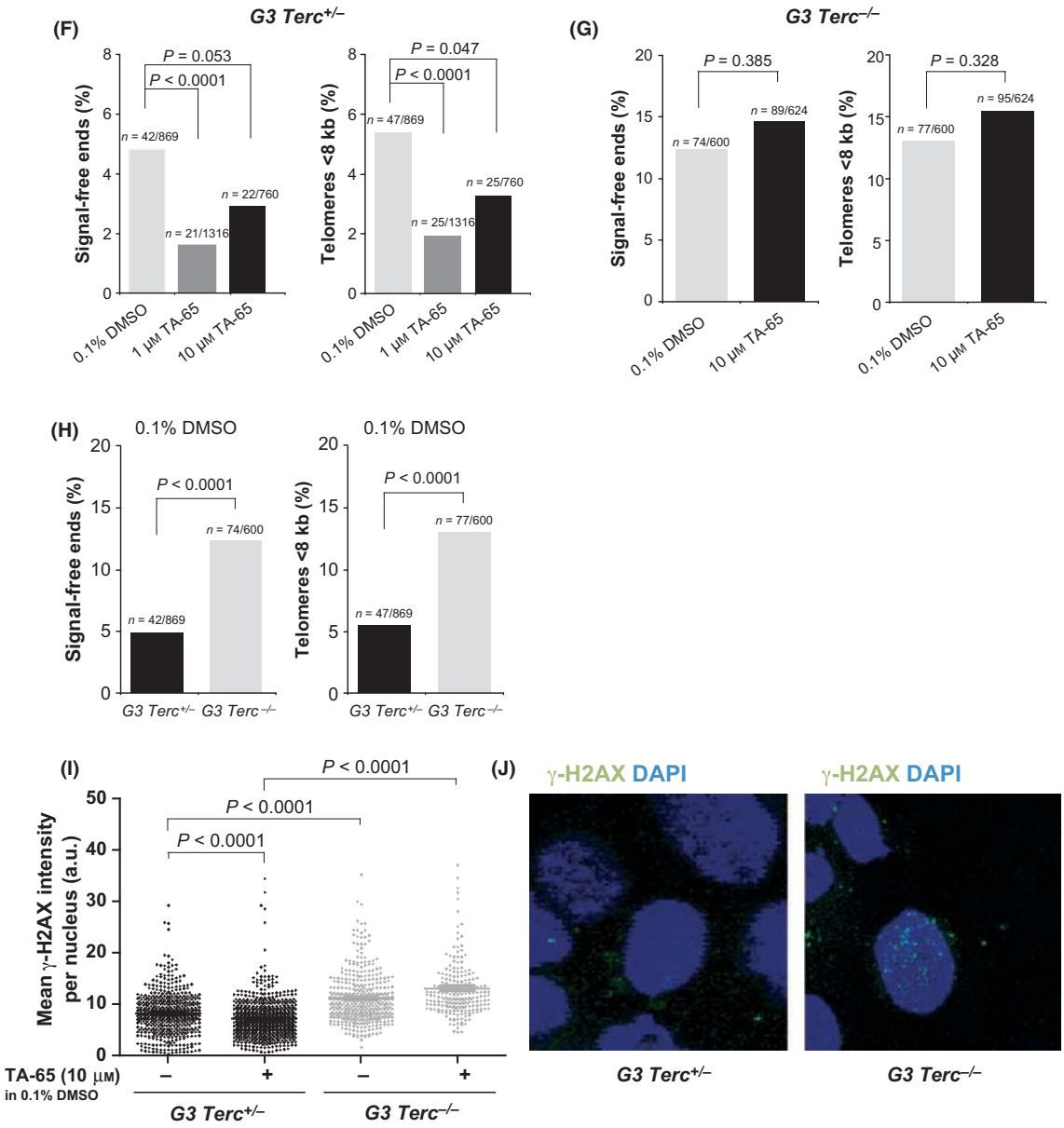

Fig. 1 Continued.

the shortest telomeres, which are the known preferred substrates of telomerase (Bianchi & Shore, 2007; Sabourin *et al.*, 2007), in an *ex vivo* model haploinsufficient for telomerase. To this end, we crossed *Terc*$^{+/-}$ female mice with G2 *Terc*$^{-/-}$ male mice to generate littermate populations of MEFs that were either G3 *Terc*$^{-/-}$ or G3 *Terc*$^{+/-}$ (hereafter referred to as G3 *Terc*$^{-/-}$ or G3 *Terc*$^{+/-}$ MEFs, respectively). The G3 progeny of these crosses inherit a set of chromosomes with short telomeres from the male *Terc*$^{-/-}$ parent and a set of chromosomes with normal telomeres from the female *Terc*$^{+/-}$ parent (Fig. 1A, scheme). Noteworthy that only the G3 *Terc*$^{+/-}$ progeny will inherit a copy of the *Terc* gene and, thereafter, is telomerase proficient (Fig. 1A). Using a telomere repeat amplification protocol assay (TRAP), we confirmed that reintroduction of the *Terc* allele successfully reconstituted telomerase activity in G3 *Terc*$^{+/-}$ cells, while G3 *Terc*$^{-/-}$ littermates persisted telomerase negative (Figs 1B and S1). Importantly, 10 μM of TA-65 significantly increased telomerase TRAP activity at 24 h post-treatment in G3 *Terc*$^{+/-}$ MEFs haploinsufficient for the telomerase RNA component, and this effect was lost 5 days post-treatment (Figs 1B,C and S1), possibly owing to fast kinetics of the compound or to the existence of negative feedback mechanisms. The observed telomerase stimulation is consistent with previous results with human keratinocytes (Harley *et al.*, 2010). These results

demonstrate that TA-65 is capable of activating telomerase by approximately 2-fold in primary MEFs haploinsufficient for telomerase activity.

The absence of telomerase in MEFs leads, among other phenotypes, to an increase in the percentage of short telomeres and 'signal-free ends' and the correlated appearance of chromosomal instability (Blasco *et al.*, 1997; Herrera *et al.*, 1999; Samper *et al.*, 2001a; Cayuela *et al.*, 2005). By using the quantitative telomere fluorescence *in situ* hybridization (Q-FISH) assay, we could observe that control telomerase reconstituted G3 *Terc*$^{+/-}$ cells treated with 0.1% DMSO present a significant decrease in 'signal-free' ends (12.3–4.8%; Fig. 1D–H) and critically short telomeres (telomeres with < 8 kb length) compared to similarly treated G3 *Terc*$^{-/-}$ littermates (12.8–5.4% Fig. 1D–H). Treatment of telomerase-proficient G3 *Terc*$^{+/-}$ cells with TA-65 during 5 days at concentrations of 1 or 10 μM resulted in an additional decrease in the percentage of 'signal-free ends' to 1.6% and 2.9%, and short telomeres to 1.9% and 3.3%, respectively, compared to their control situation (0.1% DMSO) (Fig. 1D,F). In marked contrast, TA-65-treated G3 telomerase-deficient *Terc*$^{-/-}$ littermate MEFs presented similar number of short telomeres or 'signal-free ends' confirming the telomerase-

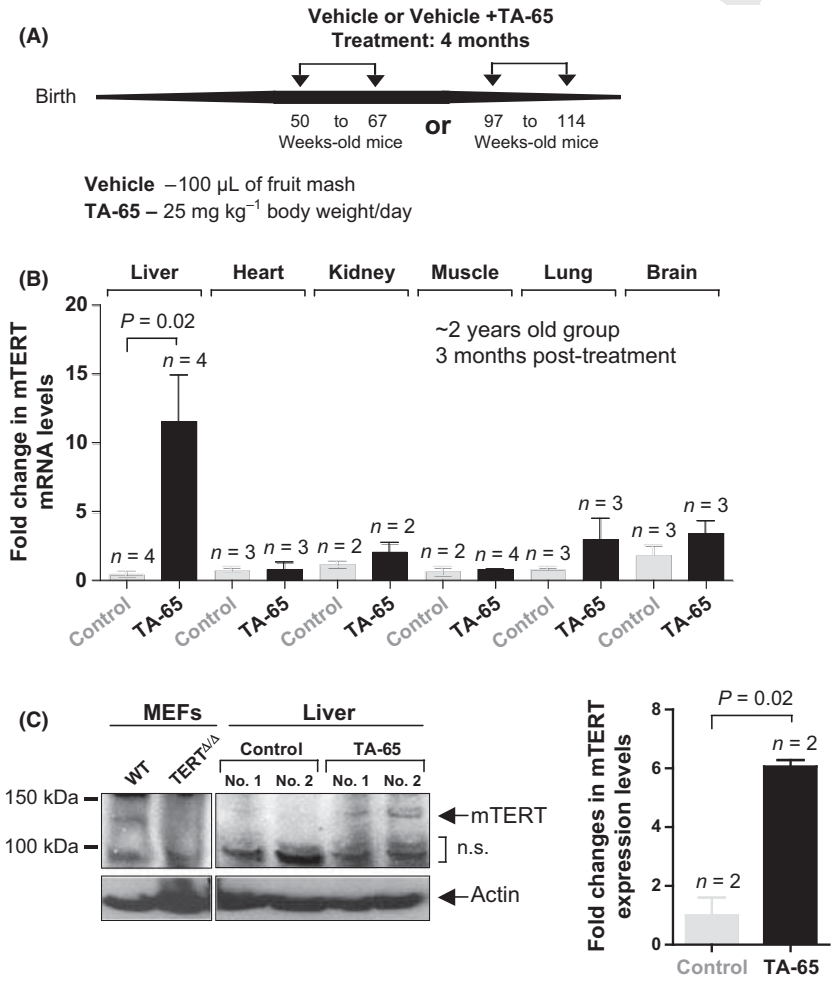

COLOR

Fig. 2 TA-65 treatment of mice leads to increased TERT expression *in vivo*. (A) Scheme of the TA-65 treatment plan. (B) Fold change in mouse telomerase reverse transcriptase (mTERT) mRNA levels in different tissues from TA-65-treated mice of the 2-year-old group compared to untreated controls at 3 month post-treatment. mTERT mRNA values were normalized to actin. Student's *t*-test was used for statistical comparisons. (C) Fold change in mTERT protein levels in liver extracts from 2-year-old mice treated or not with TA-65 (NS: nonspecific band) using an mTERT antibody previously validated by us (Martinez *et al.*, 2010)). As controls, mTERT protein expression is detected in wild-type mouse embryonic fibroblasts (MEFs) but not in TERT$^{-/-}$ MEFs (Liu *et al.*, 2000). Quantification of mTERT expression is presented in the right panel (fold changes in TERT levels compared to the values obtained in the control situation (without TA-65)). The quantification was made with Scion Image Software. Student's *t*-test was used for statistical comparisons. (D) Fold change in JunB mRNA levels at 3 months post-treatment in different tissues from 2-year-old TA-65-treated mice compared to age-matched untreated controls. JunB mRNA values were normalized to actin. (E) Fold change in c-Myc mRNA levels 3 months post-treatment in different tissues of 2-year-old TA-65-treated mice compared to age-matched untreated controls. c-Myc mRNA values were normalized to actin. Student's *t*-test was used for statistical comparisons. (F) Percentage of c-Myc-positive cells, quantified from at least four independent mice. Measurements were realized postmortem in cancer-free mice. Student's *t*-test was used for statistical comparisons. At least five high-power fields (×100) were used per independent mice (around 3000 cells scored per mice, AxioVision was used for image analysis). (G) Representative IHC of c-Myc staining in either control or TA-65-treated 2-year-old female mice. (H) Hypothetical model of action of TA-65 based in ours and previous results.

dependent mechanism of action of TA-65 (Fig. 1E,G). Additionally, a significantly increased average telomere length was observed in G3 *Terc*$^{+/-}$ cells when treated with 10 μM of TA-65 (37.87–42.68 kb, Fig. 1D). The presence of short or uncapped telomeres results in higher cellular levels of gamma-H2AX, an indicator of activation of a DNA damage response (Martinez *et al.*, 2010). In line with this, control *G3 Terc*$^{-/-}$ MEFs showed higher levels of nuclear gamma-H2AX compared to *G3 Terc*$^{+/-}$ cells (Fig. 1I and representative image in Fig. 1J). Interestingly, TA-65 treatment at the 10-μM dose decreased the levels of nuclear gamma-H2AX specifically in telomerase-proficient *G3 Terc*$^{+/-}$ cells but not in telomerase-deficient *G3 Terc*$^{-/-}$ MEFs, demonstrating that the beneficial effects of TA-65 treatment on preventing DNA damage are dependent on telomerase activity (Fig. 1I,J).

Together these results suggest that the mechanism of action of TA-65 in its capability to decrease the percentage of short telomeres, of 'signal-free ends', as well as of DNA damage, requires the presence of an active telomerase complex.

Dietary supplementation of TA-65 increases TERT expression in some tissues and rescues short telomeres in mice

Telomere attrition and the accumulation of short telomeres are parallel to the aging process in humans and mice, being a probable cause of the appearance of age-related pathologies (Harley *et al.*, 1990; Canela *et al.*, 2007; Jiang *et al.*, 2008; Calado & Young, 2009). Short telomeres are therefore both an indicator and a possible cause of health-span decay with age either in humans and mice. Following the above-described results with MEFs, we set to address whether a dietary supplementation with TA-65 could similarly lead to detectable changes on telomere dynamics *in vivo*. To this end, we fed two cohorts of

COLOR

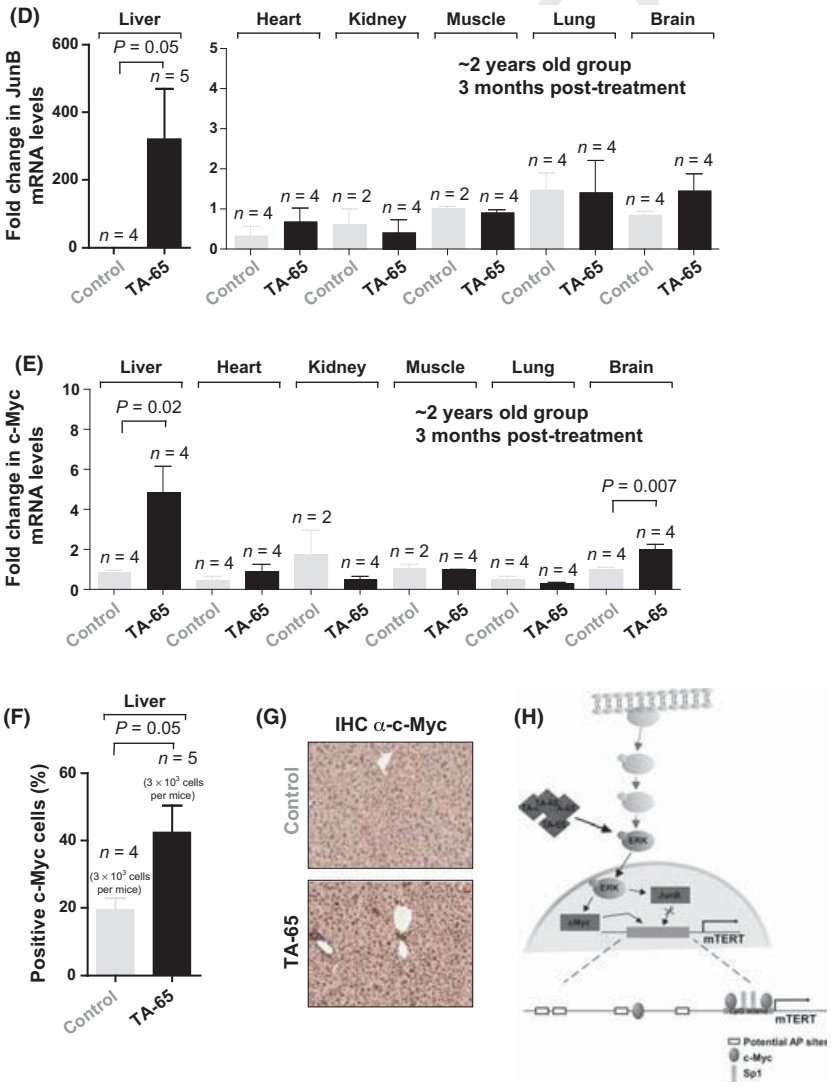

Fig. 2 Continued.

mature or old female mice (1 or 2 years old, respectively) with control vehicle (*fruit mash*) or vehicle *plus* TA-65 (final concentration of 25 mg kg^{-1} body weight/day) for 4 months (scheme in Fig. 2A, and detailed information in Methods). Treated mice demonstrated a complete tolerance to the administration of the *vehicle* or *vehicle+TA-65* as no deaths or other overt pathologies related to treatment were observed during this period. In line with this, body weight was maintained and comparable between the different mouse cohorts throughout the treatment period (Fig. S2).

It has been previously described that treatment of $CD8^+$ T lymphocytes with a similar telomerase activator compound (TAT2) leads to an 8-fold increase in human telomerase reverse transcriptase mRNA levels (Fauce *et al.*, 2008). To follow the effects of TA-65 dietary supplementation *in vivo*, we examined mouse telomerase reverse transcriptase (mTERT) mRNA levels in different tissues from the 2-year-old TA-65-treated or control cohorts at 3 months post-treatment. Notably, TA-65 treatment of 2-year-old mice resulted in a significant 10-fold increase in mTERT mRNA (Fig. 2B) and protein (Fig. 2C) levels in the liver as determined 3 month post-treatment. Mouse telomerase reverse transcriptase mRNA levels were also modestly increased in other tissues from these mice including kidney, lung and brain, although these increases did not reach statistical significance (Fig. 2B). Of note, the same patterns were observed in the 1-year-old mouse cohort (Fig. S3A). Interestingly, increased levels of mTERT in the liver of both 1- and 2-year-old TA-65-treated mice correlated with an increase in mRNA levels of JunB (Figs 2D and S3A) and c-Myc (Figs 2E and S3A), two transcription factors regulated by the MAPK pathway (Gupta *et al.*, 1993; Lefloch *et al.*, 2008), which is a known potential mediator of TA-65 action (Fauce *et al.*, 2008). Higher levels of c-Myc in the liver were confirmed by IHC in the 2-year-old group of mice, at the time of death (Fig. 2F,G). Of note, TA-65 did not altered significantly the levels of targets of the Wnt (CD44 and CyclinD1) or TGFβ (Fibronectin, Klf4, or p16) pathways (Fig. S4), further supporting that TA-65-dependent telomerase activation occurs through transcription factors regulated by the MAPK pathway, which may directly or indirectly regulate the mTERT promoter [hypothetical mechanism in Fig. 2H, based on our current findings and previous results (Wang *et al.*, 1998; Greenberg *et al.*, 1999; Chang & Karin, 2001; Inui *et al.*, 2001; Takakura *et al.*, 2005; Pericuesta *et al.*, 2006)].

To address the *in vivo* effect of TA-65 treatment on telomerase-mediated telomere elongation, we measured telomere length in blood samples from the 1- and 2-year-old controls and TA-65-treated groups, 3 months after the dietary supplementation period ending. Telomere length was assessed from peripheral blood leukocytes by using a high-throughput (HT) Q-FISH technique optimized for blood samples (Canela *et al.*, 2007). Average telomere length was not significantly increased in the 1- or 2-year-old TA-65-treated groups compared to the untreated controls (Fig. 3A,C). Interestingly, we observed a significant decrease in very short telomeres (telomeres below 2, 3 and 4 kb, Fig. 3B,D) in the 1- and 2-year-old TA-65-treated groups at 3 months post-treatment, indicating a significant and consistent capacity of TA-65 to promote rescue of short telomeres both *in vitro* (MEFs) and *in vivo* (mice). A similar scenario has been previously described in a study assessing the role of TA-65 in humans, where a reduced percentage of cells with short telomeres appeared concomitant with minimal effects in the mean telomere length (Harley *et al.*, 2010).

TA-65 treatment enhances health span in female mice

Previous studies have demonstrated that the shortest telomeres are causal of reduced cell viability (Hemann *et al.*, 2001b; Hao *et al.*, 2005) and that a stable and enforced expression of telomerase leads to an improved health span, accompanied by an extension of lifespan, possibly through the rescue of short telomeres in mice (Tomas-Loba *et al.*, 2008). As TA-65 influences the percentage of cellular short telomeres through the activation of telomerase, we were interested in addressing whether this compound could have an impact on health and/or lifespan in the treated mice.

The aging process can be evaluated by studying some of the so-called biomarkers of aging. One established indicator of aging in mice is glucose intolerance and insulin resistance, which increase with age (Bailey & Flatt, 1982; Guarente, 2006). Importantly, TA-65 administration during 4 months significantly improved the capacity to uptake glucose after a glucose pulse (area under the curve) in the 1-year-old treated mice compared to the control groups at 6 and 12 months post-treatment (Fig. 4A,D; Methods). Furthermore, 1-year-old TA-65-treated mice presented a tendency to show lower levels of blood insulin 6 months post-treatment which, together with the glucose levels at fasting, resulted in a tendency to have a better homeostasis model assessment of insulin resistance (HOMA-IR) score at 6 months post-treatment (Fig. 4B,C) (Heikkinen *et al.*, 2007). Of note, although we observed a better glucose uptake at 12 months post-treatment with TA-65 in the 1-year-old group (Fig. 4D), this was not accompanied by lower basal insulin levels or by a better HOMA-IR score; a similar situation was observed 6 months post-treatment in the 2-year-old TA-65-treated group (Fig. 4E–I). These findings may suggest that a discontinued TA-65 intake could result in an attenuation of some health-span improvements [a situation in agreement with previous observations (Fauce *et al.*, 2008)], and/or that old mice are less refractory to TA-65 treatment.

Liver steatosis is caused by lipid accumulation within hepatocytes both in humans and in mice. Despite being a relatively benign condition, when combined with inflammation it may progress to serious liver disease (Feldstein *et al.*, 2003; Higuchi & Gores, 2003). Although mouse liver steatosis models involve usually intake of a high-fat diet (and subsequent diet-induced obesity) (Pfluger *et al.*, 2008), this condition may also occur in aged mice under standard diet conditions (Kelder *et al.*, 2007). As expected, lipid droplets were found in liver sections of both control and TA-65-treated mice at the time of death (Fig. 4J).

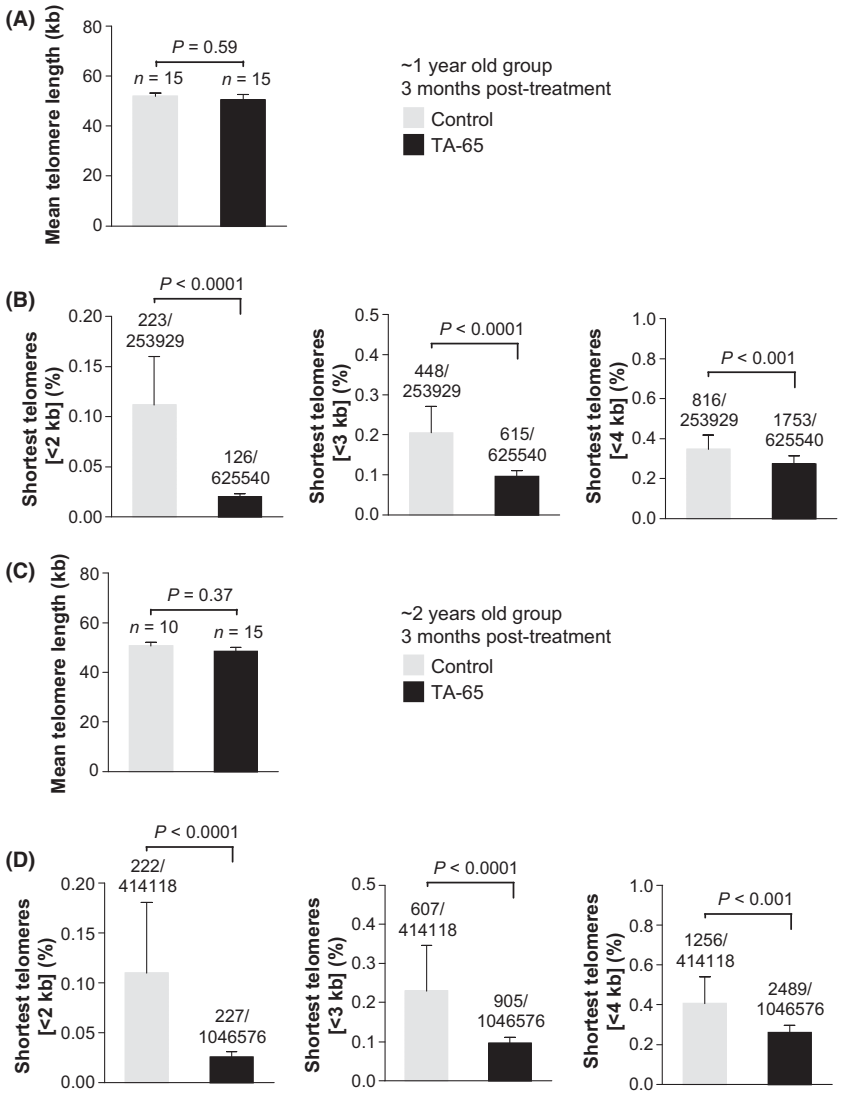

Fig. 3 TA-65 rescues short telomeres *in vivo* A, C. High-throughput-quantitative telomere fluorescence *in situ* hybridization telomere length analysis of the 1-year-old (A) or 2-year-old (C), control or TA-65-treated group, 3 month post-treatment. B, D. Percentage of short telomeres (fraction of telomeres presenting a size below 2, 3 or 4 kb), 3 month post-treatment, in the 1-year-old (B) or 2-year-old (D) group of mice. Data are given as mean ± SEM.

Interestingly, control mice presented the strongest accumulation of fat in the liver at older ages comparing to the TA-65-treated cohorts, which, together with the previous results, could indicate a liver protective action of TA-65 (Fig. 4J).

Other well-established biomarkers of aging are the loss of the epidermal and subcutaneous adipose skin layers (Shimokata *et al.*, 1989; Tomas-Loba *et al.*, 2008). The weakness of the skin barrier associates with infections and deficient water exchange. TA-65 treatment resulted in a significant increase in subcutaneous fat content and epidermal layer in the 1-year-old group of mice (Fig. 5A,C and representative image in Fig. 5B), but did not significantly change these parameters in the 2-year-old groups (Fig. 5A,C), compared to the untreated controls. In line with an improved epithelial fitness, TA-65 treatment increased the *in vitro* wound-healing capacity of keratinocytes (Fig. 5D) as well as significantly accelerated hair regrow *in vivo* upon plucking of old mice (Fig. 5E and representative image in Fig. 5F). Moreover, the epidermis of TA-65-treated mice showed significantly more proliferating cells (Ki67-positive cells; Fig. 5G and representative image in Fig. 5H) together with significantly reduced numbers of TUNEL-positive apoptotic cells (Fig. 5I and representative image at Fig. 5J). Similar results were obtained in the lung (Fig. S5A–D) but not in the liver (Fig. S5E–H), suggesting that the capacity of TA-65 to stimulate proliferation *in vivo* may be tissue-dependent.

Bone loss, which results from the imbalance between osteoclast and osteoblasts, is also a common finding with increasing age both in mice and in humans, leading to age-related bone fragility (Ferguson *et al.*, 2003). Bone density was improved in the 2-year-old TA-65-treated group compared to their controls without TA-65 supplementation (measurements at the time of death, Fig. 5K).

Previous findings demonstrated that TA-65 uptake leads to significant changes in blood or immune parameters in humans (Fauce *et al.*, 2008; Harley *et al.*, 2010). Table 1 summarizes the haematological analysis of either 1- and 2-year-old control mice compared to TA-65-treated groups. Although no significant dif-

COLOR

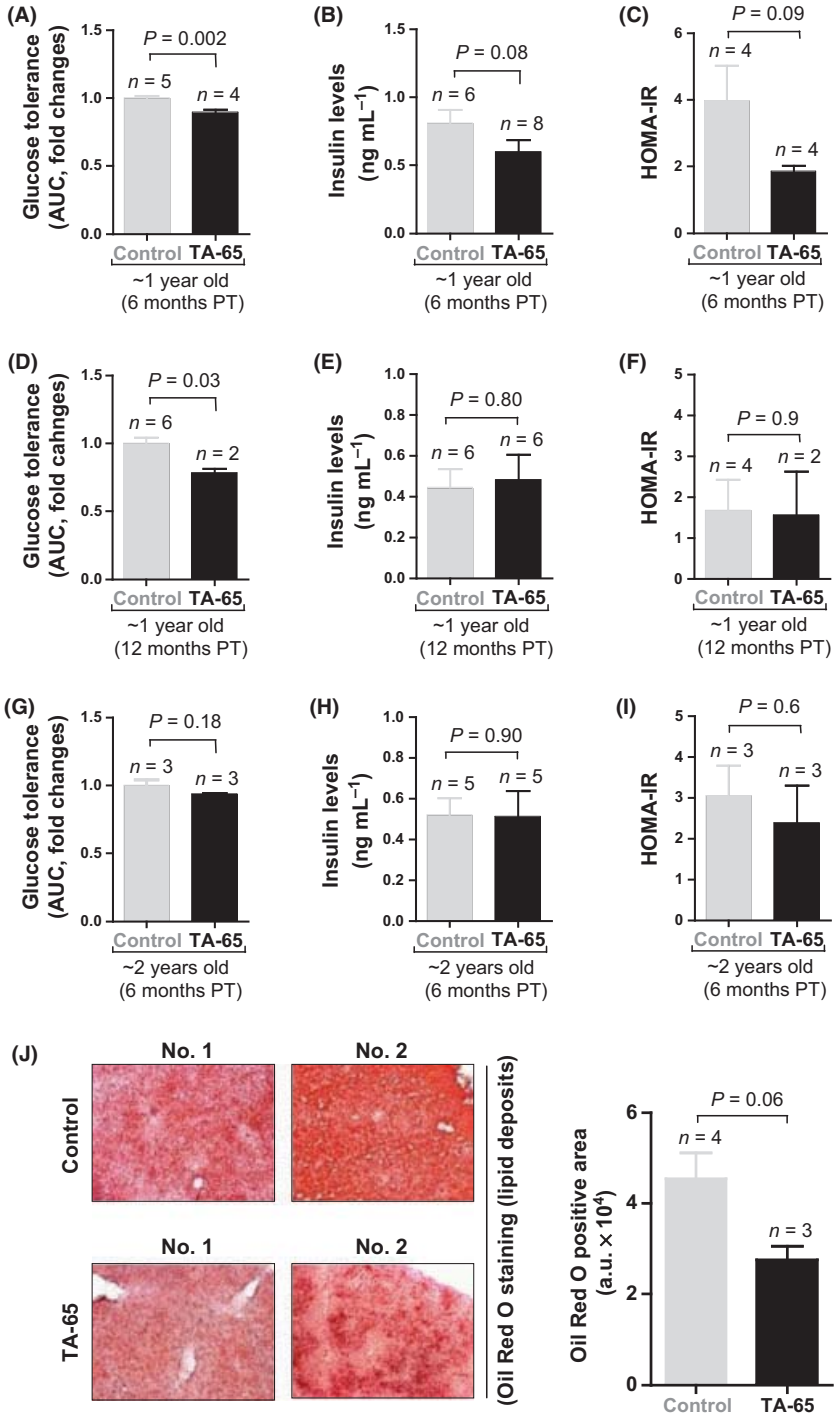

Fig. 4 TA-65 treatment increases metabolic fitness. (A, D, G) Glucose tolerance measured as fold changes to the area under the curve at the indicated time post-treatment in the 1- or 2-year-old cohort of mice. (B, E, H) Insulin levels at the indicated times post-treatment in the 1- or 2-year old cohort of mice. (C, F, I) Homeostatic model assessment scores at the indicated time post-treatment in the 1- or 2-year-old cohort of mice. TA-65 supplemented mice present a better score at 6 months post-treatment, indicating a better metabolic rate. (J) Oil red O staining of lipid droplets in frozen liver sections from either controls or TA-65-treated mice on a standard diet. Measures were realized postmortem in cancer-free mice. Quantification of Oil Red O area is presented in the right panel (five images per mice; Photoshop CS3 and Scion Image software were used for image analysis).

ferences were observed in the 1-year-old group, we could observe significant differences in the level of red blood cells (RBC), hemoglobin, and platelets in the TA-65-treated 2-year-old group compared to age-matched cohorts. The absence of differences in the 1-year-old group could be because the blood analysis was performed at the time of death, which occurred

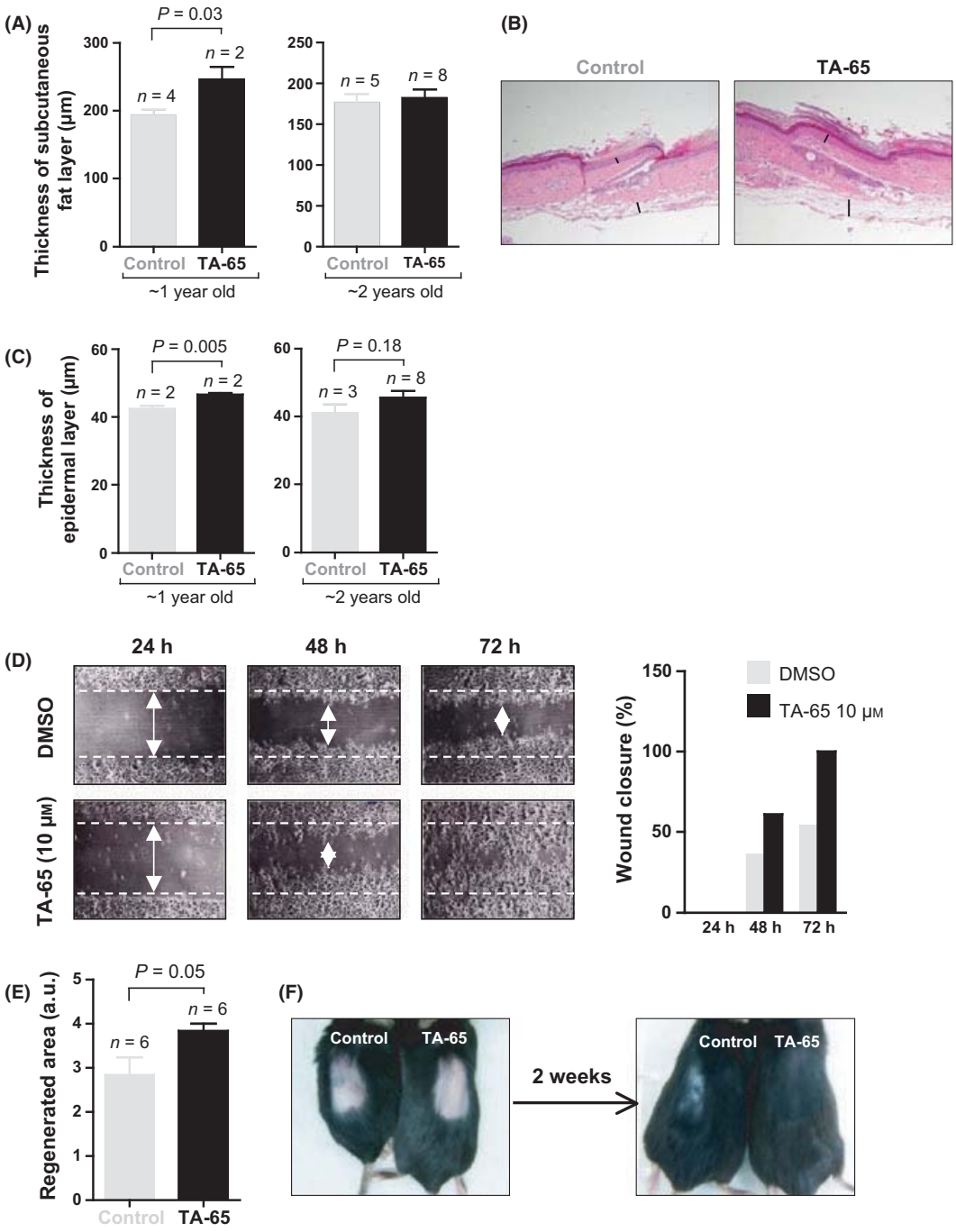

COLOR

Fig. 5 TA-65 treatment delays some age-associated pathologies. (A) Thickness of the subcutaneous fat layer at the time of death in 1- and 2-year-old mice treated or nontreated with TA-65. (B) Representative images of subcutaneous fat and epidermal layers in mice feed with vehicle or vehicle plus TA-65. (C) Thickness of the skin epidermal layer at the time of death in 1- and 2-year-old mice treated or nontreated with TA-65. (D) Stimulation of wound closure in neonatal human epidermal keratinocytes cells incubated in the presence of TA-65. Images were taken after incubating for 24, 48 and 72 h. Wound closure was calculated and is presented in the right panel. (E) Hair regrowth capacity was quantified in arbitrary units (a.u., see Methods) 14 day after plucking. Fisher's exact test was used for statistical analysis. Experiments were carried 12 months after the ending to the TA-65 supplementation period in the 1-year-old cohort of mice. Six independent mice were used. (F) Representative images of hair regrowth. Images were acquired in anesthetized female mice of the 1-year-old group before and 14 days after hair plucking. (G) Percentage of Ki67-positive cells in the epidermis (tail skin) of TA-65-treated or untreated (control) mice. Student's *t*-test was used for statistical assessments. At least six high-power fields (HPF, ×100) were used per independent mouse and around 2000 skin epidermis cells were scored per mouse. (H) Representative Ki67 immunohistochemistry images of skin epidermis (tail) from TA-65-treated or untreated (control) mice. (I) Percentage of TUNEL-positive (Apoptag detection kit) cells in the epidermis (tail skin) of TA-65-treated or untreated (control) mice. Student's *t*-test was used for statistical assessments. At least six HPF (×100) were used per independent mouse and around 2000 skin epidermis cells were scored per mice. (J) Representative TUNEL stained images of skin from TA-65-treated or untreated (control) mice. (K) Femur bone mineral density (BMD femur) measured at the time of death in the 2-year-old cohorts treated with or nontreated with TA-65.

COLOR

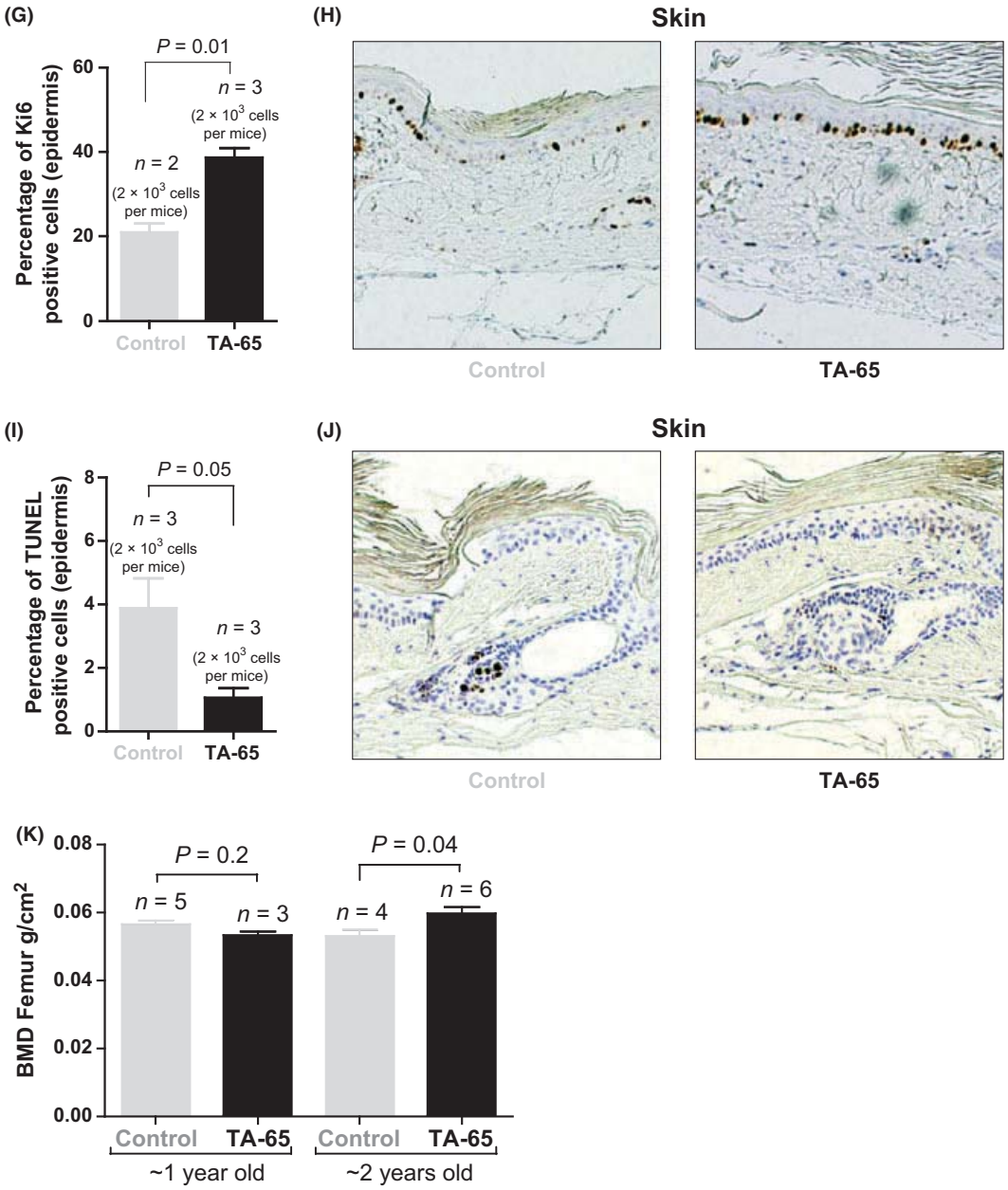

Fig. 5 Continued.

much after the treatment period in the 1-year-old group, where the effect of TA-65 has been already partially lost.

These results demonstrate that TA-65 *per se* can modestly but significantly enhance overall organ fitness of both mature (1 year old) and old (2 years old) female mice.

TA-65 intake does not impact on mean or maximum longevity of female mice

The known impact of telomerase in aging and cancer lead us to address whether TA-65 supplementation could have any beneficial or undesirable effects on mouse survival and cancer incidence, respectively. Recent evidences demonstrate that enforced expression of telomerase either from the germline (together with enforced expression of tumor suppressors) or ectopically in adult/old mice leads to a significant extension of both mean and maximum lifespan [(Tomas-Loba *et al.*, 2008) and unpublished data].

Analysis of the Kaplan–Meier survival curves of control vs. TA-65-treated female mice demonstrated no significant effects of TA-65 intake on survival (Fig. 6A,B). Accordingly, TA-65 administration for 4 months did not change statistically the mean or maximal lifespan of female mice under our experimental conditions.

Table 1 Values for relevant blood/immune variables among TA-65-treated and controls, in both aged cohorts

Blood/Immune variables	Control 1 year old (time of death)	TA-65 1 year old (time of death)	*t*-test	Control 2 years old (time of death)	TA-65 2 years old (time of death)	*t*-test
WBC, 10^9 L^{-1}	7.4	5.4	0.1	8.1	4.5	*
LYM, %	49.6	50.0	n.s.	41.4	36.9	n.s.
MI, %	2.5	4.7	n.s.	6.8	4.2	n.s.
GR, %	47.9	44.9	n.s.	51.7	62.2	n.s.
RBC, 10^{12} L^{-1}	7.1	7.1	n.s.	4.8	6.3	**
HGB, g dL^{-1}	10.1	10.0	n.s.	7.6	9.2	**
HCT, %	24.3	23.9	n.s.	21.5	26.6	**
PLT, 10^9 L^{-1}	354	289	n.s.	292	587	*

TA-65 intake does not increase cancer incidence

A disadvantage of mTERT potentiation could be associated with its capacity to favor the proliferation of cancerous cells in murine models (Gonzalez-Suarez *et al.*, 2001; Artandi *et al.*, 2002; Canela *et al.*, 2004; McKay *et al.*, 2008; Tomas-Loba *et al.*, 2008; Rafnar *et al.*, 2009). To address whether TA-65 supplemented diet had undesirable long-term side effects, we performed a pathological analysis of all female mice under treatment and controls at the time of death. We observed that TA-65-treated mice presented a similar incidence of malignant cancers at the time of death, with a tendency to show decreased sarcomas and slightly increased lymphomas (Fig. 6C,D). Moreover, although we observed an increased incidence of cancer in the liver of TA-65-treated mice (were TA-65 treatment resulted in a 10-fold increase in TERT expression) compared to control mice, these differences did not reach statistical significance (Fig. 6D).

Discussion

Strategies to extend healthspan conditions with lifetime extension have been the target of scientific investigation for decades. From the preliminary studies describing the effects of caloric restriction, which evolve to detailed characterizations of pathways and potential targets resulting in recent conceivable treatments, the outcome has been continually focused in a healthier organismal living (Guarente & Kenyon, 2000; Hayflick, 2000; Kirkwood & Austad, 2000; Kenyon, 2010).

Here, we characterize a small-molecule compound (TA-65) extracted from the roots of a medicinal Chinese plant used, among other things, to 'protect' the immune system or 'preserve' the liver (Shen *et al.*, 2006; Clement-Kruzel *et al.*, 2008; Mao *et al.*, 2009). We demonstrate here that TA-65 leads to a significant rescue of short telomeres through telomerase activation in MEFs haploinsufficient for the telomerase RNA component. Indeed, TA-65 treatment increases proliferation and mobilization potential of mouse keratinocytes *in vitro*, a situation mimicking telomerase overexpression (Greider, 1998; Cerezo *et al.*, 2003). Recently, Fauce *et al.* (2008)demonstrated that TAT2, a similar molecule, have beneficial effects in the activation of $CD8^+$ T lymphocytes from HIV-infected patients where they observe an increase in the proliferative potential and enhancement of cytokine/chemokine production.

The use of TA-65 as a treatment to improve health span in humans has been tested in past few years, where subjects took

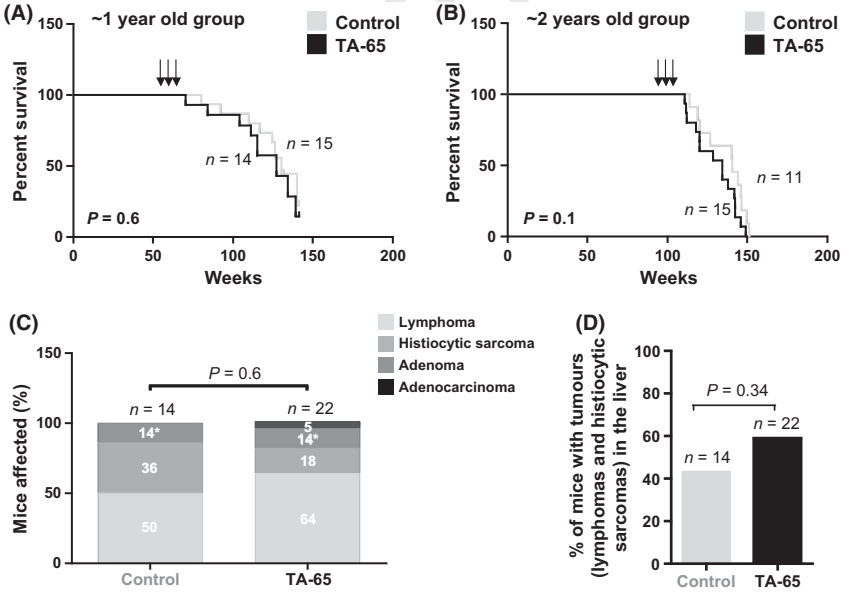

Fig. 6 Dietary supplementation of TA-65 has no effect on lifespan in female mice. (A, B) Survival curves of the indicated control of TA-65-treated 1- and 2-year-old mouse cohorts. Alive mice are plotted as a vertical line. The Log rank test was used for statistical analysis. (C) Percentage of mice with the indicated tumor at their time of death. [* Of note that 100% (two mice) and 33% (one mice) of the mice presenting adenomas also present lymphomas in the control and TA-65 situations, respectively]. (D) Percentage of cancer penetrance (histiocytic sarcomas and lymphomas) in the liver of the indicated mice cohorts.

part in an open label comprehensive dietary supplementation program, which included a TA-65 dose of 10–50 mg daily (Harley *et al.*, 2010). Report analysis of the first treatment year has been recently released, demonstrating high tolerability and some beneficial effects in humans after treatment periods ranging from 3 to 12 months (Harley *et al.*, 2010). We have now assessed the specific effects of TA-65 in a blinded study of two cohorts of 1-year-old (mature) or 2-year-old (old) female mice where an adjusted dose of TA-65 was administrated daily for 4 months. Similar to humans, TA-65 treatment in mice resulted in a similar rescue of short telomeres in leukocytes at 3 month post-treatment. Interestingly, we observed that, at least in mice, the liver is one of the main targets of TA-65 treatment, where it leads to a > 10-fold increase in TERT RNA levels compared to nontreated age-matched cohorts. Furthermore, this increase in mTERT mRNA levels is accompanied by increased c-Myc and JunB mRNA levels. These results enforce the previous idea that TA-65 regulates telomerase at the transcription level, probably through the regulation of the MAPK pathway (Fauce *et al.*, 2008). Whether or not TA-65 could regulate post-transcriptionally the levels of telomerase in the liver or other tissues has not been assessed here or elsewhere, although this is improbable in the case of mouse telomerase because some mTERT post-translational modifications such as phosphorylation is mediated through the AKT pathway, which seems not to be influenced by TA-65 (Kang *et al.*, 1999; Gomez-Garcia *et al.*, 2005; Fauce *et al.*, 2008).

We further show here that TA-65-dependent telomerase activation results in a better organ fitness as demonstrated by the improved scores at the glucose tolerance test. These enhancements could be related to the TA-65-dependent ERK pathway activation in the liver and subsequent telomerase expression, which have been shown to mediate the glucose tolerance and insulin response (Tomas-Loba *et al.*, 2008). Moreover, ERK signal is silenced by the activation of the p38 MAPK, which responds to external damage signals arising usually with aging progression and oxidative damage accumulation, and result in age-related insulin insensitivity and glucose intolerance (Kyriakis & Avruch, 2001; Au *et al.*, 2003; Li *et al.*, 2007; Bluher *et al.*, 2009). TA-65-supplemented mice also present modest but significant enhancement of the subcutaneous and epidermal thickness, as well as higher bone density, representative of an overall fitness status improvement. A similar situation has been previously observed in mice overexpressing the telomerase catalytic subunit (Tomas-Loba *et al.*, 2008). Analysis of the blood parameters also demonstrated that 2-year-old TA-65-treated mice present higher levels of RBC and hemoglobin compared to the control cohorts. The decrease in such parameters is a regular situation experienced during aging progression in healthy old mice and could be related to RBC fragility and deficient regulation of the stem cell pools (Ewing & Tauber, 1964; Finch & Foster, 1973; Tyan, 1980, 1982a,b; Xing *et al.*, 2006). Importantly, improved health span of TA-65-treated mice is not accompanied by increased cancer incidence, which may be related to the fact that TERT levels are very modestly increased in all tissues tested except for the liver. Alternatively, telomerase enhancement in adult (1 year old) or very old mice (2 year old) may have beneficial effects without increasing cancer incidence because older organisms are more refractory to proliferative stimuli.

Finally, the results obtained here with MEFs haploinsufficient for telomerase activity suggest that the beneficial effects of TA-65 treatment in rescuing critically short telomeres and DNA damage are likely mediated by the telomerase pathway. This goes in line with recent data from our group showing that systemic mTERT overexpression from the germline leads to rescue of short telomeres and of DNA damage and to protection from aging-associated pathologies (Tomas-Loba *et al.*, 2008). Similarly, re-expression of TERT in mice that were already aged because of TERT deficiency can rescue telomere length and delay aging in these mice (Jaskelioff *et al.*, 2010). Finally, TERT increase expression may also have beneficial effects on aging through its potential ability to activate the Wnt pathway (Park *et al.*, 2009).

Here, we provide evidence on the role of TA-65 in a healthy aging improvement but not survival (either mean or maximum longevity) in female mice. The balance between health enhancement and longevity do not always correlate. Indeed, if a long-lived mammalian organism presents regularly health benefits (Berryman *et al.*, 2008; Tomas-Loba *et al.*, 2008), the opposite as shown to be potentially untrue (Herranz & Serrano, 2010). Of importance is the fact that we feed our mice cohorts for a limited period of time (4 months), being the impact of the compound shown to be partially lost during the absence period (Fauce *et al.*, 2008); even though, we show that some phenotypic rescues (such as the hair regrowth) can be maintained longer after TA-65 uptake conclusion. We cannot discard that a longer or constant dietary supplementation of TA-65 could also impact on lifespan or cancer. In conclusion, here we described new findings on the potential therapeutic use of TA-65, delineating for the first time its mechanism of action and organismal response.

Methods

Formulation of TA-65

TA-65 was obtained from *TA Sciences*. TA-65 is a > 95% pure single chemical entity as judged by HPLC and NMR (data not shown), which was isolated from a proprietary extract of the dried root of *Astragalus membranaceus* (Harley *et al.*, 2010). TA-65 was dissolved in DMSO at 1- or 10-mM stock concentration (1000× final concentration).

Mice, cells, and treatments

All G2 $Terc^{-/-}$ and $Terc^{+/-}$ mice used in this study were of the same identical genetic background (C57BL6). Third-generation G3 $Terc^{-/-}$ and G3 $Terc^{+/-}$ littermate mouse embryos were derived from crossing G2 $Terc^{-/-}$ with $Terc^{+/-}$ mice (Fig. 1A). Genotyping was performed by Southern blotting as described

(Blasco *et al.*, 1997). Mice were maintained at the Spanish National Cancer Centre (CNIO) under specific pathogen-free conditions in accordance with the recommendations of the Federation of European Laboratory Animal Science Associations.

Mouse embryonic fibroblasts were prepared from day 13.5 embryos as described (Blasco *et al.*, 1997). Two independent TA-65 treatments were performed using independent MEF cultures. G3 *Terc*$^{-/-}$ and G3 *Terc*$^{+/-}$ primary MEF (passage 1) were cultured for 6 days in Dulbecco's modified Eagle's medium (Gibco, Paisley, UK) supplemented with 10% fetal bovine serum and antibiotic/antimycotic at 37 °C/5% CO_2. Fresh TA-65 was added to the media at a final concentration of 1 or 10 μM every 24–48 h, along with change of media, and cells were passaged at day 2 and 5. Control cells were treated with 0.1% DMSO.

Aged cohorts of female mice were obtained directly from Harlan Laboratories. Both 1- and 2-year-old groups were aged under standard conditions and present 100% C57BL/6JOlaHsd background. Mice were conditioned in a pathogen-free area of CNIO after arrival, in accordance with the recommendations of the Federation of European Laboratory Animal Science Associations. Half of the mice were supplemented with 25 mg of TA-65 *per* kg of mouse body weight *per* day, mixed in 100 μL of fruit mash, for 4 months. Fruit mash alone was supplemented to the control cohorts (100 μL, with the same periodicity as treatment groups). Mice were daily inspected by an authorized animal facility supervisor, before and after TA-65 treatment. Mice were sacrificed when presenting signs of illness or tumors in accordance with the Guidelines for Humane Endpoints for Animals Used in Biomedical Research.

Telomere repeat amplification protocol

Telomerase activity in G3 *Terc*$^{-/-}$ and G3 *Terc*$^{+/-}$ MEF was measured by TRAP as described previously (Blasco *et al.*, 1997). Protein extracts of HCT116 cells served as a positive control. As negative controls, protein extracts were treated with 5-μg RNase for 10 min at 30 °C before performing the TRAP assay. Radioactive gels were exposed to BioMax MS films (Kodak) for at least 12 h at –80 °C. Quantification was performed on digitalized films, using ImageJ software (NIH). The mean intensity of each lane after background subtraction was calculated, normalized by the dilution factor of the applied protein extract, and expressed as folds relative to the corresponding DMSO-treated cells.

Q-FISH and HT QFISH

At 70% confluence, primary MEFs (passage 3) were incubated with 0.1 mg mL^{-1} Colcemide (Gibco) at 37 °C for 4 h to induce metaphases. Cells were then harvested and fixed in methanol/acetic acid (3:1). Metaphases were spread on glass slides and dried overnight, and Q-FISH was performed using a PNA-telomeric probe as described previously (Herrera *et al.*, 1999; Samper *et al.*, 2000).

Metaphases were analyzed with a fluorescence microscope (DMRA2; Leica, Wetzlar, Germany), and images were captured with a COHU CCD camera (San Diego, CA, USA) using the Leica Q-FISH software. Fluorescence intensity of telomeres was quantified by spot IOD analysis using the TFL-TELO software (provided by P. Landsdorp, Vancouver, Canada) and normalized to the fluorescence intensity of fluorescent beads (Molecular Probes, Carlsbad, CA, USA).

High-throughput-quantitative telomere fluorescence *in situ* hybridization was performed as previously described (Canela *et al.*, 2007). Briefly, blood was extracted at the indicated time points after TA-65 treatment was finished. Peripheral blood leukocytes were plated on a clear bottom black-walled 96-well plate. Telomere length values were analyzed using individual telomere spots (> 5000 per sample) corresponding to the specific binding of a Cy3-labeled telomeric probe. Fluorescence intensities were converted into kilobase as previously described (McIlrath *et al.*, 2001; Canela *et al.*, 2007).

Quantitative real-time RT–PCR

Total RNA from liver was extracted with Trizol (Life Technologies). Samples were treated with DNase *I* before reverse transcription using random primers and Superscript Reverse Transcriptase (Life Technologies), following the manufacturer's guidelines. The primers used were as follows:

Actin-For: GGCACCACACCTTCTACAATG;
Actin-Rev: GTGGTGGTGAAGCTGTAG;
TERT-For: GGATTGCCACTGGCTCCG;
TERT-Rev: TGCCTGACCTCCTCTTGTGAC;
JunB-For: AGC CGC CTC CCG TCT ACA CCA;
JunB-Rev GCC GCT TTC GCTCCA CTT TGA TG;
c-Myc-For: ATGCCCCTCAACGTGAACTTC;
c-Myc-Rev: CGCAACATAGGATGGAGAGCA;
CyclinD1-For: TGCGCCCTCCGTATCTTAC;
CyclinD1-Rev: ATCTTAGAGGCCACGAACATGC;
CD44-For: CAGCCTACTGGAGATCAGGATGA;
CD44-Rev: GGAGTCCTTGGATGAGTCTCGA;
p16-For*:* CGTACCCCGATTCAGGTGAT;
p16-Rev*:* TTGAGCAGAAGAGCTGCTACGT;
Klf4-For: GCGAACTCACACAGGCGAGAAACC;
Klf4-Rev: TCGCTTCCTCTTCCTCCGACACA;
Fibronectin-For: TACCAAGGTCAATCCACACCCC;
Fibronectin-Rev: CAGATGGCAAAAGAAAGCAGAGG.

Student's *t*-test was performed on the $\Delta\Delta C_t$ as previously recommended (Yuan *et al.*, 2006; Matheu *et al.*, 2007).

Histological analyses

We performed c-Myc (sc-764; Santa Cruz biotechnology) Ki67 (M7249, clone TEC-3) and TUNEL (ApopTag Detection Kit) staining on paraformaldehyde-fixed, paraffin-embedded sections (AxioVision and Scion Image software were used for image analysis; quantitation of immunostaining was determined by counting the number of peroxidase stained nuclei over the total

number of haematoxylin-stained nuclei) and oil red O staining (fat cells) on liver frozen sections. Samples were processed and acquired under identical conditions.

For complete blood cell counts, we collected blood samples just before euthanasia. Data represents information collected from, at least, five mice. Counts were done using an Abacus Junior Vet System.

Glucose tolerance tests, insulin levels, and HOMA-IR

Glucose tolerance test and analysis were performed as described elsewhere (Moynihan *et al.*, 2005). Mice were fasted for at least 6 h and injected intraperitoneally with a 50% dextrose solution (2 g kg^{-1} body weight).

Blood insulin levels were measured with an Ultra-Sensitive Mouse Insulin ELISA Kit (Crystal Chem Inc. no 90080), following the manufacturers protocol. Mice were fasted for at least 6 h prior to blood insulin analysis. HOMA-IR was calculated as previously described (Matthews *et al.*, 1985; Heikkinen *et al.*, 2007).

Bone density, skin measurements, and cell migration

Bone mineral density was measured in the femur of female mice postmortem using a dual energy X-ray absorptiometry scan device. Subcutaneous fat and epidermal layers measurements were performed as previously described (Tomas-Loba *et al.*, 2008). ImageJ software was used for skin length measurements.

Cell migration assays were performed on neonatal human epidermal keratinocytes (HEKn). Briefly, a confluent monolayer of HEKn was scraped with a sterile pipette tip. Migration into the wound was scored after 24, 48, or 72 h in the presence of DMSO or TA-65 (10 μM). ImageJ software was used for length measurements.

Hair regrowth assay was performed and quantified as previously described (Matheu *et al.*, 2007). Briefly, dorsal hair was removed by plucking from a square of approximately 1.5 × 1.5 cm. Hair regrowth was scored two weeks later and a semi-quantitative assessment using an arbitrary scale from one to four (where four represents complete hair regeneration).

Statistical analyses

Statistical significances were calculated using GraphPad Prism 5 software. An unpaired student's *t*-test was used to calculate statistical significances of telomerase activity (TRAP), mRNA expression levels, protein levels, IHC quantification, glucose tolerance, insulin levels, HOMA-IR, skin measurements, and bone mineral density. Statistical analysis of hair regrowth experiments was assessed with Fisher's exact test. Statistical significances of differences in overall telomere length were determined by Wilcoxon-Mann–Whitney rank sum test. For statistical analyses of percentage of short telomeres and pathological analysis at the time of death, a chi-square test was used. Finally, a Log rank test was used for survival comparisons between cohorts.

Acknowledgments

We thank R. Serrano for mouse care and J. Flores for pathology analyses. We thank Comparative Pathology Unit at CNIO for technical assistance. M.A. Blasco's laboratory is funded by the Spanish Ministry of Science and Innovation (MICINN), the European Union (GENICA, TELOMARKER), the European Reseach Council (ERC Advance Grants), the Körber European Science Award and the Fundacion Lilly Preclinical Award to M.A. Blasco. Maria A. Blasco acts as consultant and holds stock in Life Length, S.L., a biotechnology company based on measuring telomeres as an indication of health status and biological age of samples.

Author contributions

M.A.B conceived the idea. B.B. performed most of the experiments of the paper. K.S. performed the TA-65 administration and performed the analyses shown in Figs 1D–G and 5D. E.V. performed telomere length determinations (Fig. 3). A.T. performed the TRAP assays (Figs 1B and S1). M.A.B and B.B. wrote the paper.

References

Armanios MY, Chen JJ, Cogan JD, Alder JK, Ingersoll RG, Markin C, Lawson WE, Xie M, Vulto I, Phillips JA 3rd, Lansdorp PM, Greider CW, Loyd JE (2007) Telomerase mutations in families with idiopathic pulmonary fibrosis. *N. Engl. J. Med.* **356**, 1317–1326.

Artandi SE, Alson S, Tietze MK, Sharpless NE, Ye S, Greenberg RA, Castrillon DH, Horner JW, Weiler SR, Carrasco RD, DePinho RA (2002) Constitutive telomerase expression promotes mammary carcinomas in aging mice. *Proc. Natl. Acad. Sci. USA* **99**, 8191–8196.

Au WS, Kung HF, Lin MC (2003) Regulation of microsomal triglyceride transfer protein gene by insulin in HepG2 cells: roles of MAPKerk and MAPKp38. *Diabetes* **52**, 1073–1080.

Bailey CJ, Flatt PR (1982) Hormonal control of glucose homeostasis during development and ageing in mice. *Metabolism* **31**, 238–246.

Berryman DE, Christiansen JS, Johannsson G, Thorner MO, Kopchick JJ (2008) Role of the GH/IGF-1 axis in lifespan and healthspan: lessons from animal models. *Growth Horm. IGF Res.* **18**, 455–471.

Bianchi A, Shore D (2007) Increased association of telomerase with short telomeres in yeast. *Genes Dev.* **21**, 1726–1730.

Blackburn EH (2001) Switching and signaling at the telomere. *Cell* **106**, 661–673.

Blasco MA, Lee HW, Hande MP, Samper E, Lansdorp PM, DePinho RA, Greider CW (1997) Telomere shortening and tumor formation by mouse cells lacking telomerase RNA. *Cell* **91**, 25–34.

Bluher M, Bashan N, Shai I, Harman-Boehm I, Tarnovscki T, Avinaoch E, Stumvoll M, Dietrich A, Kloting N, Rudich A (2009) Activated Ask1-MKK4-p38MAPK/JNK stress signaling pathway in human omental fat tissue may link macrophage infiltration to whole-body insulin sensitivity. *J. Clin. Endocrinol. Metab.* **94**, 2507–2515.

Calado RT, Young NS (2009) Telomere diseases. *N. Engl. J. Med.* **361**, 2353–2365.

Canela A, Martin-Caballero J, Flores JM, Blasco MA (2004) Constitutive expression of tert in thymocytes leads to increased incidence and dissemination of T-cell lymphoma in Lck-Tert mice. *Mol. Cell. Biol.* **24**, 4275–4293.

Canela A, Vera E, Klatt P, Blasco MA (2007) High-throughput telomere length quantification by FISH and its application to human population studies. *Proc. Natl. Acad. Sci. USA* **104**, 5300–5305.

Cayuela ML, Flores JM, Blasco MA (2005) The telomerase RNA component Terc is required for the tumour-promoting effects of Tert overexpression. *EMBO Rep.* **6**, 268–274.

Cerezo A, Stark HJ, Moshir S, Boukamp P (2003) Constitutive overexpression of human telomerase reverse transcriptase but not c-myc blocks terminal differentiation in human HaCaT skin keratinocytes. *J. Invest. Dermatol.* **121**, 110–119.

Chang L, Karin M (2001) Mammalian MAP kinase signalling cascades. *Nature* **410**, 37–40.

Clement-Kruzel S, Hwang SA, Kruzel MC, Dasgupta A, Actor JK (2008) Immune modulation of macrophage pro-inflammatory response by goldenseal and Astragalus extracts. *J. Med. Food.* **11**, 493–498.

Ewing KL, Tauber OE (1964) Hematological Changes in Aging Male C57bl/6 Jax Mice. *J. Gerontol.* **19**, 165–167.

Fauce SR, Jamieson BD, Chin AC, Mitsuyasu RT, Parish ST, Ng HL, Kitchen CM, Yang OO, Harley CB, Effros RB (2008) Telomerase-based pharmacologic enhancement of antiviral function of human CD8+ T lymphocytes. *J. Immunol.* **181**, 7400–7406.

Feldstein AE, Canbay A, Angulo P, Taniai M, Burgart LJ, Lindor KD, Gores GJ (2003) Hepatocyte apoptosis and fas expression are prominent features of human nonalcoholic steatohepatitis. *Gastroenterology* **125**, 437–443.

Ferguson VL, Ayers RA, Bateman TA, Simske SJ (2003) Bone development and age-related bone loss in male C57BL/6J mice. *Bone* **33**, 387–398.

Finch CE, Foster JR (1973) Hematologic and serum electrolyte values of the C57BL-6J male mouse in maturity and senescence. *Lab. Anim. Sci.* **23**, 339–349.

Flores I, Cayuela ML, Blasco MA (2005) Effects of telomerase and telomere length on epidermal stem cell behavior. *Science* **309**, 1253–1256.

Flores I, Canela A, Vera E, Tejera A, Cotsarelis G, Blasco MA (2008) The longest telomeres: a general signature of adult stem cell compartments. *Genes Dev.* **22**, 654–667.

Gomez-Garcia L, Sanchez FM, Vallejo-Cremades MT, de Segura IA, del Campo Ede M (2005) Direct activation of telomerase by GH via phosphatidylinositol 3'-kinase. *J. Endocrinol.* **185**, 421–428.

Gonzalez-Suarez E, Samper E, Ramirez A, Flores JM, Martin-Caballero J, Jorcano JL, Blasco MA (2001) Increased epidermal tumors and increased skin wound healing in transgenic mice overexpressing the catalytic subunit of telomerase, mTERT, in basal keratinocytes. *EMBO J.* **20**, 2619–2630.

Greenberg RA, O'Hagan RC, Deng H, Xiao Q, Hann SR, Adams RR, Lichtsteiner S, Chin L, Morin GB, DePinho RA (1999) Telomerase reverse transcriptase gene is a direct target of c-Myc but is not functionally equivalent in cellular transformation. *Oncogene* **18**, 1219–1226.

Greider CW (1998) Telomerase activity, cell proliferation, and cancer. *Proc. Natl. Acad. Sci. USA* **95**, 90–92.

Greider CW, Blackburn EH (1985) Identification of a specific telomere terminal transferase activity in Tetrahymena extracts. *Cell* **43**, 405–413.

Guarente L (2006) Sirtuins as potential targets for metabolic syndrome. *Nature* **444**, 868–874.

Guarente L, Kenyon C (2000) Genetic pathways that regulate ageing in model organisms. *Nature* **408**, 255–262.

Gupta S, Seth A, Davis RJ (1993) Transactivation of gene expression by Myc is inhibited by mutation at the phosphorylation sites Thr-58 and Ser-62. *Proc. Natl. Acad. Sci. USA* **90**, 3216–3220.

Hao LY, Armanios M, Strong MA, Karim B, Feldser DM, Huso D, Greider CW (2005) Short telomeres, even in the presence of telomerase, limit tissue renewal capacity. *Cell* **123**, 1121–1131.

Harley CB (2005) Telomerase therapeutics for degenerative diseases. *Curr. Mol. Med.* **5**, 205–211.

Harley CB, Futcher AB, Greider CW (1990) Telomeres shorten during ageing of human fibroblasts. *Nature* **345**, 458–460.

Harley CB, Liu W, Blasco M, Vera E, Andrews WH, Briggs LA, Raffaele JM (2010) A natural product telomerase activator as part of a health maintenance program. *Rejuvenation Res.* **???**, ???. 21

Hayflick L (2000) The future of ageing. *Nature* **408**, 267–269.

Heikkinen S, Argmann CA, Champy MF, Auwerx J (2007) Evaluation of glucose homeostasis. *Curr. Protoc. Mol. Biol.* Chapter 29, Unit 29B 23.

Hemann MT, Rudolph KL, Strong MA, DePinho RA, Chin L, Greider CW (2001a) Telomere dysfunction triggers developmentally regulated germ cell apoptosis. *Mol. Biol. Cell* **12**, 2023–2030.

Hemann MT, Strong MA, Hao LY, Greider CW (2001b) The shortest telomere, not average telomere length, is critical for cell viability and chromosome stability. *Cell* **107**, 67–77.

Herranz D, Serrano M (2010) Impact of Sirt1 on mammalian aging. *Aging (Albany NY)* **2**, 315–316.

Herrera E, Samper E, Martin-Caballero J, Flores JM, Lee HW, Blasco MA (1999) Disease states associated with telomerase deficiency appear earlier in mice with short telomeres. *EMBO J.* **18**, 2950–2960.

Higuchi H, Gores GJ (2003) Mechanisms of liver injury: an overview. *Curr. Mol. Med.* **3**, 483–490.

Inui T, Shinomiya N, Fukasawa M, Kuranaga N, Ohkura S, Seki S (2001) Telomerase activation and MAPK pathways in regenerating hepatocytes. *Hum. Cell* **14**, 275–282.

Jaskelioff M, Muller FL, Paik JH, Thomas E, Jiang S, Adams AC, Sahin E, Kost-Alimova M, Protopopov A, Cadinanos J, Horner JW, Maratos-Flier E, Depinho RA (2010) Telomerase reactivation reverses tissue degeneration in aged telomerase-deficient mice. *Nature* **???**, ???. 22

Jiang H, Schiffer E, Song Z, Wang J, Zurbig P, Thedieck K, Moes S, Bantel H, Saal N, Jantos J, Brecht M, Jeno P, Hall MN, Hager K, Manns MP, Hecker H, Ganser A, Dohner K, Bartke A, Meissner C, Mischak H, Ju Z, Rudolph KL (2008) Proteins induced by telomere dysfunction and DNA damage represent biomarkers of human aging and disease. *Proc. Natl. Acad. Sci. USA* **105**, 11299–11304.

Kang SS, Kwon T, Kwon DY, Do SI (1999) Akt protein kinase enhances human telomerase activity through phosphorylation of telomerase reverse transcriptase subunit. *J. Biol. Chem.* **274**, 13085–13090.

Kelder B, Boyce K, Kriete A, Clark R, Berryman DE, Nagatomi S, List EO, Braughler M, Kopchick JJ (2007) CIDE-A is expressed in liver of old mice and in type 2 diabetic mouse liver exhibiting steatosis. *Comp. Hepatol.* **6**, 4.

Kenyon CJ (2010) The genetics of ageing. *Nature* **464**, 504–512.

Kirkwood TB, Austad SN (2000) Why do we age? *Nature* **408**, 233–238.

Kyriakis JM, Avruch J (2001) Mammalian mitogen-activated protein kinase signal transduction pathways activated by stress and inflammation. *Physiol. Rev.* **81**, 807–869.

de Lange T (2005) Shelterin: the protein complex that shapes and safeguards human telomeres. *Genes Dev.* **19**, 2100–2110.

Lefloch R, Pouyssegur J, Lenormand P (2008) Single and combined silencing of ERK1 and ERK2 reveals their positive contribution to growth signaling depending on their expression levels. *Mol. Cell. Biol.* **28**, 511–527.

Li G, Barrett EJ, Barrett MO, Cao W, Liu Z (2007) Tumor necrosis factor-alpha induces insulin resistance in endothelial cells via a p38

mitogen-activated protein kinase-dependent pathway. *Endocrinology* **148**, 3356–3363.

Liu Y, Snow BE, Hande MP, Yeung D, Erdmann NJ, Wakeham A, Itie A, Siderovski DP, Lansdorp PM, Robinson MO, Harrington L (2000) The telomerase reverse transcriptase is limiting and necessary for telomerase function in vivo. *Curr. Biol.* **10**, 1459–1462.

Mao XQ, Yu F, Wang N, Wu Y, Zou F, Wu K, Liu M, Ouyang JP (2009) Hypoglycemic effect of polysaccharide enriched extract of *Astragalus membranaceus* in diet induced insulin resistant C57BL/6J mice and its potential mechanism. *Phytomedicine* **16**, 416–425.

Martinez P, Thanasoula M, Carlos AR, Gomez-Lopez G, Tejera AM, Schoeftner S, Dominguez O, Pisano DG, Tarsounas M, Blasco MA (2010) Mammalian Rap1 controls telomere function and gene expression through binding to telomeric and extratelomeric sites. *Nat. Cell Biol.* **12**, 768–780.

Matheu A, Maraver A, Klatt P, Flores I, Garcia-Cao I, Borras C, Flores JM, Vina J, Blasco MA, Serrano M (2007) Delayed ageing through damage protection by the Arf/p53 pathway. *Nature* **448**, 375–379.

Matthews DR, Hosker JP, Rudenski AS, Naylor BA, Treacher DF, Turner RC (1985) Homeostasis model assessment: insulin resistance and beta-cell function from fasting plasma glucose and insulin concentrations in man. *Diabetologia* **28**, 412–419.

McIlrath J, Bouffler SD, Samper E, Cuthbert A, Wojcik A, Szumiel I, Bryant PE, Riches AC, Thompson A, Blasco MA, Newbold RF, Slijepcevic P (2001) Telomere length abnormalities in mammalian radiosensitive cells. *Cancer Res.* **61**, 912–915.

McKay JD, Hung RJ, Gaborieau V, Boffetta P, Chabrier A, Byrnes G, Zaridze D, Mukeria A, Szeszenia-Dabrowska N, Lissowska J, Rudnai P, Fabianova E, Mates D, Bencko V, Foretova L, Janout V, McLaughlin J, Shepherd F, Montpetit A, Narod S, Krokan HE, Skorpen F, Elvestad MB, Vatten L, Njolstad I, Axelsson T, Chen C, Goodman G, Barnett M, Loomis MM, Lubinski J, Matyjasik J, Lener M, Oszutowska D, Field J, Liloglou T, Xinarianos G, Cassidy A, Vineis P, Clavel-Chapelon F, Palli D, Tumino R, Krogh V, Panico S, Gonzalez CA, Ramon Quiros J, Martinez C, Navarro C, Ardanaz E, Larranaga N, Kham KT, Key T, Bueno-de-Mesquita HB, Peeters PH, Trichopoulou A, Linseisen J, Boeing H, Hallmans G, Overvad K, Tjonneland A, Kumle M, Riboli E, Zelenika D, Boland A, Delepine M, Foglio M, Lechner D, Matsuda F, Blanche H, Gut I, Heath S, Lathrop M, Brennan P (2008) Lung cancer susceptibility locus at 5p15.33. *Nat. Genet.* **40**, 1404–1406.

Mitchell JR, Wood E, Collins K (1999) A telomerase component is defective in the human disease dyskeratosis congenita. *Nature* **402**, 551–555.

Moynihan KA, Grimm AA, Plueger MM, Bernal-Mizrachi E, Ford E, Cras-Meneur C, Permutt MA, Imai S (2005) Increased dosage of mammalian Sir2 in pancreatic beta cells enhances glucose-stimulated insulin secretion in mice. *Cell Metab.* **2**, 105–117.

Park JI, Venteicher AS, Hong JY, Choi J, Jun S, Shkreli M, Chang W, Meng Z, Cheung P, Ji H, McLaughlin M, Veenstra TD, Nusse R, McCrea PD, Artandi SE (2009) Telomerase modulates Wnt signalling by association with target gene chromatin. *Nature* **460**, 66–72.

Pericuesta E, Ramirez MA, Villa-Diaz A, Relano-Gines A, Torres JM, Nieto M, Pintado B, Gutierrez-Adan A (2006) The proximal promoter region of mTERT is sufficient to regulate telomerase activity in ES cells and transgenic animals. *Reprod. Biol. Endocrinol.* **4**, 5.

Pfluger PT, Herranz D, Velasco-Miguel S, Serrano M, Tschop MH (2008) Sirt1 protects against high-fat diet-induced metabolic damage. *Proc. Natl. Acad. Sci. USA* **105**, 9793–9798.

Rafnar T, Sulem P, Stacey SN, Geller F, Gudmundsson J, Sigurdsson A, Jakobsdottir M, Helgadottir H, Thorlacius S, Aben KK, Blondal T, Thorgeirsson TE, Thorleifsson G, Kristjansson K, Thorisdottir K, Ragnarsson R, Sigurgeirsson B, Skuladottir H, Gudbjartsson T, Isaksson HJ, Einarsson GV, Benediktsdottir KR, Agnarsson BA, Olafsson K, Salvarsdottir A, Bjarnason H, Asgeirsdottir M, Kristinsson KT, Matthiasdottir S, Sveinsdottir SG, Polidoro S, Hoiom V, Botella-Estrada R, Hemminki K, Rudnai P, Bishop DT, Campagna M, Kellen E, Zeegers MP, de Verdier P, Ferrer A, Isla D, Vidal MJ, Andres R, Saez B, Juberias P, Banzo J, Navarrete S, Tres A, Kan D, Lindblom A, Gurzau E, Koppova K, de Vegt F, Schalken JA, van der Heijden HF, Smit HJ, Termeer RA, Oosterwijk E, van Hooij O, Nagore E, Porru S, Steineck G, Hansson J, Buntinx F, Catalona WJ, Matullo G, Vineis P, Kiltie AE, Mayordomo JI, Kumar R, Kiemeney LA, Frigge ML, Jonsson T, Saemundsson H, Barkardottir RB, Jonsson E, Jonsson S, Olafsson JH, Gulcher JR, Masson G, Gudbjartsson DF, Kong A, Thorsteinsdottir U, Stefansson K (2009) Sequence variants at the TERT-CLPTM1L locus associate with many cancer types. *Nat. Genet.* **41**, 221–227.

Sabourin M, Tuzon CT, Zakian VA (2007) Telomerase and Tel1p preferentially associate with short telomeres in *S. cerevisiae*. *Mol. Cell* **27**, 550–561.

Samper E, Goytisolo FA, Slijepcevic P, van Buul PP, Blasco MA (2000) Mammalian Ku86 protein prevents telomeric fusions independently of the length of TTAGGG repeats and the G-strand overhang. *EMBO Rep.* **1**, 244–252.

Samper E, Flores JM, Blasco MA (2001a) Restoration of telomerase activity rescues chromosomal instability and premature aging in $Terc^{-/-}$ mice with short telomeres. *EMBO Rep.* **2**, 800–807.

Samper E, Goytisolo FA, Menissier-de Murcia J, Gonzalez-Suarez E, Cigudosa JC, de Murcia G, Blasco MA (2001b) Normal telomere length and chromosomal end capping in poly(ADP-ribose) polymerase-deficient mice and primary cells despite increased chromosomal instability. *J. Cell Biol.* **154**, 49–60. **23**

Shen P, Liu MH, Ng TY, Chan YH, Yong EL (2006) Differential effects of isoflavones, from *Astragalus membranaceus* and *Pueraria thomsonii*, on the activation of PPARalpha, PPARgamma, and adipocyte differentiation in vitro. *J. Nutr.* **136**, 899–905.

Shimokata H, Tobin JD, Muller DC, Elahi D, Coon PJ, Andres R (1989) Studies in the distribution of body fat: I. Effects of age, sex, and obesity. *J. Gerontol.* **44**, M66–M73.

Siegl-Cachedenier I, Flores I, Klatt P, Blasco MA (2007) Telomerase reverses epidermal hair follicle stem cell defects and loss of long-term survival associated with critically short telomeres. *J. Cell Biol.* **179**, 277–290.

Takakura M, Kyo S, Inoue M, Wright WE, Shay JW (2005) Function of AP-1 in transcription of the telomerase reverse transcriptase gene (TERT) in human and mouse cells. *Mol. Cell. Biol.* **25**, 8037–8043.

Teixeira MT, Arneric M, Sperisen P, Lingner J (2004) Telomere length homeostasis is achieved via a switch between telomerase- extendible and -nonextendible states. *Cell* **117**, 323–335.

Tomas-Loba A, Flores I, Fernandez-Marcos PJ, Cayuela ML, Maraver A, Tejera A, Borras C, Matheu A, Klatt P, Flores JM, Vina J, Serrano M, Blasco MA (2008) Telomerase reverse transcriptase delays aging in cancer-resistant mice. *Cell* **135**, 609–622.

Tsakiri KD, Cronkhite JT, Kuan PJ, Xing C, Raghu G, Weissler JC, Rosenblatt RL, Shay JW, Garcia CK (2007) Adult-onset pulmonary fibrosis caused by mutations in telomerase. *Proc. Natl. Acad. Sci. USA* **104**, 7552–7557.

Tyan ML (1980) Marrow colony-forming units: age-related changes in responses to anti-theta-sensitive helper/suppressor stimuli. *Proc. Soc. Exp. Biol. Med.* **165**, 354–360.

Tyan ML (1982a) Age-related increase in erythrocyte oxidant sensitivity. *Mech. Ageing Dev.* **20**, 25–32.

Tyan ML (1982b) Effect of age on the intrinsic regulation of murine hemopoiesis. *Mech. Ageing Dev.* **19**, 15–20.

Vulliamy T, Marrone A, Goldman F, Dearlove A, Bessler M, Mason PJ, Dokal I (2001) The RNA component of telomerase is mutated in autosomal dominant dyskeratosis congenita. *Nature* **413**, 432–435.

Wang J, Xie LY, Allan S, Beach D, Hannon GJ (1998) Myc activates telomerase. *Genes Dev.* **12**, 1769–1774.

Xing Z, Ryan MA, Daria D, Nattamai KJ, Van Zant G, Wang L, Zheng Y, Geiger H (2006) Increased hematopoietic stem cell mobilization in aged mice. *Blood* **108**, 2190–2197.

Yamaguchi H, Calado RT, Ly H, Kajigaya S, Baerlocher GM, Chanock SJ, Lansdorp PM, Young NS (2005) Mutations in TERT, the gene for telomerase reverse transcriptase, in aplastic anemia. *N. Engl. J. Med.* **352**, 1413–1424.

Yuan JS, Reed A, Chen F, Stewart CN Jr (2006) Statistical analysis of real-time PCR data. *BMC Bioinformatics* **7**, 85.

Supporting Information

Additional supporting information may be found in the online version of this article:

Fig. S1 Representative telomerase telomere repeat amplification protocol assay in mouse embryonic fibroblasts treated with the indicated dose of TA-65 for 24 h and 5 days. A cellular extract from HCT116 cells was included as a positive control, and RNase was added in all experimental settings as negative control. IC, PCR efficiency control.

Fig. S2 Body weight of the indicated mice before or after treatment is given as mean ± SEM.

Fig. S3 (A) Fold change in mouse telomerase reverse transcriptase (mTERT) mRNA levels at 3 months post-treatment in different tissues of 1-year-old TA-65-treated mice compared to age-matched controls. Mouse telomerase reverse transcriptase mRNA values were normalized to actin. (B) Fold change in JunB mRNA levels at 3 months post-treatment in different tissues of 1-year-old TA-65-treated mice compared to age-matched nontreated controls. JunB mRNA values were normalized to actin. (C) Fold change in c-Myc mRNA levels at 3 months post-treatment in different tissues of 1-year-old TA-65-treated mice compared to age-matched nontreated controls. c-Myc mRNA values were normalized to actin.

Fig. S4 Fold changes in CD44, CyclinD1, Klf4, Fibronectin and p16 mRNA levels in liver extracts from TA-65-treated mice compared to age-matched nontreated controls. mRNA values were normalized to actin.

Fig. S5 (A) Percentage of Ki67-positive cells in the lungs of TA-65-treated or untreated (control) mice. Student's *t*-test was used for statistical assessments. At least four high-power fields (HPF) (×100) were used per independent mouse and around 24 000 lung cells were scored per mouse. (B) Representative Ki67 immunohistochemistry images of lungs from TA-65-treated or untreated (control) mice. (C) Percentage of TUNEL-positive (Apoptag detection kit) cells in the lungs of TA-65-treated or untreated (control) mice. Student's *t*-test was used for statistical assessments. At least four HPF (×100) were used per independent mouse and around 24 000 cells were scored per mouse. (D) Representative TUNEL stained images of lungs from TA-65-treated or untreated (control) mice. (E) Percentage of Ki67-positive cells in the liver of TA-65-treated or untreated (control) mice. Student's *t*-test was used for statistical assessments. At least five HPF (×100) were used per independent mouse and around 3000 hepatocytes were scored per mouse. (F) Representative Ki67 immunohistochemistry images of the liver from TA-65-treated or untreated (control) mice. (G) Percentage of TUNEL-positive (Apoptag detection kit) cells in the liver of TA-65-treated or untreated (control) mice. Student's *t*-test was used for statistical assessments. At least five HPF (×100) were used per independent mouse, and around 3000 hepatocytes were scored per mouse. (H) Representative TUNEL stained images of the liver from TA-65-treated or untreated (control) mice.

As a service to our authors and readers, this journal provides supporting information supplied by the authors. Such materials are peer-reviewed and may be re-organized for online delivery, but are not copy-edited or typeset. Technical support issues arising from supporting information (other than missing files) should be addressed to the authors.